International Journal of Mass Spectrometry 303 (2011) 199–205

Contents lists available at ScienceDirect

International Journal of Mass Spectrometry

journal homepage: www.elsevier.com/locate/ijms

Distribution into the quadrupole mass filter with round rods

F. Kashanian[a], S. Nouri[a], S. Seddighi Chaharborj[b,d,*], A.B. Mohd Rizam[c,d]

[a] Physics Group, Nuclear Science and Technology Research Institute, A.E.O.I., P.O. Box: 11365-3486 Tehran, Iran
[b] Nuclear Science Research School and Technology Research Institute (NSTRI), P.O. Box 14395-836, Tehran, Iran
[c] Department of Mathematics, Faculty of Science, Universiti Putra Malaysia, 43400 UPM, Malaysia
[d] Laboratory of Theoretical Mathematics, Institute for Mathematicsl Research, Universiti Putra Malaysia, Malaysia

ARTICLE INFO

Article history:
Received 20 November 2010
Received in revised form 1 February 2011
Accepted 2 February 2011
Available online 15 March 2011

Keywords:
Mass filter
Quadrupole
Hyperbolic rods
Round rods
Fifth order Runge–Kutta method
Stability regions
Ion trajectory

ABSTRACT

Potential field distribution of a quadrupole mass filter with circular cross-section electrodes is described. At first, using superposition principle, we calculate potential around a round rod which is subjected to a given potential. By standard separation method, we then able to obtain the potential distribution into the quadrupole mass filter with circular rods. The results are compared with those obtained with a conventional hyperbolic rod set. Also, the results show that, for the same equivalent operating point in two stability diagrams (having the same β_y) the associated modulated secular ion frequencies behavior are the same.

© 2011 Elsevier B.V. All rights reserved.

1. Introduction

Quadrupole mass filter employed in mass spectrometry was first introduced by Paul et al. [1,10]. It uses an electrical field to separate the charged particles according to their mass-to-charge ratios. The ideal quadrupole field is produced from four electrodes of hyperbolic cross-section. Normally, however, four circular rods are used to obtain the field approximately because the hyperbolic shape is difficult to machine. Several studies were done about quadrupole mass filter with round rods [2–9].

In this work, we study such device by electro dynamical calculating the problem. The paper is organized as follows. In Section (2), we study quadrupole mass filter with hyperbolic electrodes. Quadrupole mass filter with circular rods is discussed in Section (3), and in the last section we present results.

2. Quadrupole mass filter with hyperbolic rods

Quadrupole mass filter principle was established by Paul and Steinwedel [10]. It consists of four parallel hyperbolic cross-section rod electrodes as shown in Fig. 1. If opposite pairs of electrodes have steady potentials Φ_0 and $-\Phi_0$, it follows that the potential in the space between them is

$$\Phi(x, y) = c_1\Phi_0(x^2 - y^2), \tag{1}$$

where x and y are position coordinates from centerline (z-axis), c_1 is constant and

$$\Phi_0 = U_{dc} + V_{ac}\cos(\Omega t), \tag{2}$$

where U_{dc} is direct potential, U_{ac} is the zero to peak amplitude of the RF voltage, and Ω is RF angular frequency. The equation Eq. (1) satisfies the Laplace equation and boundary conditions of the system.

In each of the perpendicular directions x and y, the equation of motion for a particle of mass m and charge e in such a time varying field may be written,

$$\frac{d^2x}{d\zeta^2} + (a_x - 2q_x\cos(2\zeta))x = 0, \tag{3}$$

$$\frac{d^2y}{d\zeta^2} - (a_y - 2q_y\cos(2\zeta))y = 0, \tag{4}$$

where $\zeta = \frac{\Omega t}{2}$, and

$$a_x = -a_y = 8c_1\frac{e}{m}\times\frac{U_{dc}}{r_{0,1}^2\Omega^2} \text{ and } q_x = -q_y = 4c_1\frac{e}{m}\times\frac{V_{ac}}{r_{0,1}^2\Omega^2}. \tag{5}$$

* Corresponding author. Tel.: +60 389437958; fax: +60 389437958.
E-mail addresses: ph_1385@yahoo.co.in (F. Kashanian), seddighi@math.upm.edu.my, sseddighi2007@yahoo.com (S. Seddighi Chaharborj).

1387-3806/$ – see front matter © 2011 Elsevier B.V. All rights reserved.
doi:10.1016/j.ijms.2011.02.001

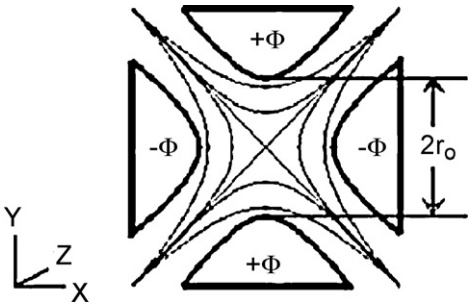

Fig. 1. Quadrupole mass filter with hyperbolic cross-section rods.

Here $r_{0,1}$ is the distance from the rod surface to the z-axis. These equations are forms of Mathieu's differential equation. The solutions of this equation are complex and discussed in literature [11]. The solutions are classified as stable and unstable. If the amplitude of oscillational motion is less than, the charged particle does not strike the rods and then its trajectory is stable. If the amplitude of oscillation is larger than, particle strikes a rod and is lost. In this case, its trajectory is unstable.

3. Quadrupole mass filter with circular rods

For obtaining the potential distribution into the quadrupole mass filter, we must, at first, calculate potential around a round rod with length L and radius a which is subjected to potential $\Phi_0/2$. By superposition principle, we can write potential of a circular rod as

$$\Phi = \Phi_1 + \Phi_2 + \Phi_3, \tag{6}$$

where Φ_1 is potential of a cylindrical rod that its upper base has potential $\Phi_0/2$, and potentials of its lower base and lateral surface are zero. Φ_2 is potential of it that its lower base has potential $\Phi_0/2$, and potentials of its upper base and lateral surface are zero. Φ_3 is potential of it when its lateral surface is subjected to potential $\Phi_0/2$, and its potentials of upper and lower bases are zero.

For calculation each of Φ's, we must solve the Laplace equation in cylindrical coordinates,

$$\frac{1}{r}\frac{\partial}{\partial r}\left(r\frac{\partial \Phi}{\partial r}\right) + \frac{1}{r^2}\frac{\partial^2 \Phi}{\partial \varphi^2} + \frac{\partial^2 \Phi}{\partial z^2} = 0, \tag{7}$$

where

$$\Phi(r, \varphi, z) = R(r)Q(\varphi)Z(z), \tag{8}$$

is general solution of potential. By following the standard separation method, we shall obtain,

$$\Phi_1(r, \varphi, z) = \sum_{n=1}^{\infty} \left(\frac{2\Phi_0}{\pi a}\right)\left(\frac{1}{k_{0n}}\right) N_0(k_{0n}r)\sinh(k_{0n}z) \times \left(\frac{C_0 \operatorname{sech}(k_{0n}L)}{N_1(k_{0n}a)}\right), \tag{9}$$

$$\Phi_2(r, \varphi, z) = \sum_{n=1}^{\infty} \left(\frac{2\Phi_0}{\pi a}\right)\left(\frac{1}{k_{0n}}\right) N_0(k_{0n}r)\left(\frac{C_0 \operatorname{sech}(k_{0n}L)}{N_1(k_{0n}a)}\right) \times (\cosh(k_{0n}z) - \sinh(k_{0n}z)\frac{\cosh(k_{0n}L)}{\sinh(k_{0n}L)}), \tag{10}$$

$$\Phi_3(r, \varphi, z) = \sum_{n=1}^{\infty} \left(\frac{\Phi_0}{n\pi}\right) k_0\left(\frac{n\pi r}{L}\right)\sin\left(\frac{n\pi z}{L}\right)\left(\frac{1-\cos(n\pi)}{k_0(\frac{n\pi a}{L})}\right), \tag{11}$$

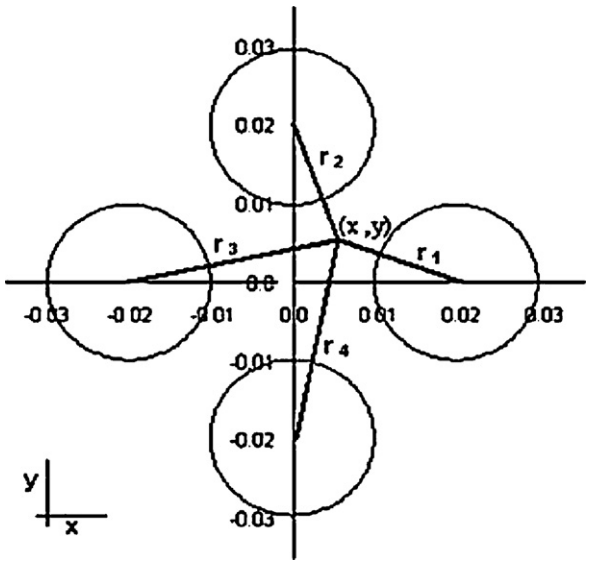

Fig. 2. Quadrupole mass filter with circular cross-section rods.

where $N(k_{0n}r)$ is the Neumann function and k_{0n}'s are zeros of Bessel function. Now, using Eq. (7) and selecting suitable position coordinates as,

$$r_1 = \{(r_{0,2} - x)^2 + y^2\}^{1/2}, \tag{12}$$

$$r_2 = \{x^2 + (r_{0,2} - y)^2\}^{1/2}, \tag{13}$$

$$r_3 = \{(r_{0,2} + x)^2 + y^2\}^{1/2}, \tag{14}$$

$$r_4 = \{x^2 + (r_{0,2} + y)^2\}^{1/2}, \tag{15}$$

where $r_{0,2}$'s are distance from centers of rods, as shown in Fig. 2.

we able to obtain the potential distribution in the space between rods to fourth order approximation as,

$$\Phi(x, y) = \Phi_0(3.8099x^2 - 3.8099y^2 + O(x^4) + O(y^4)). \tag{16}$$

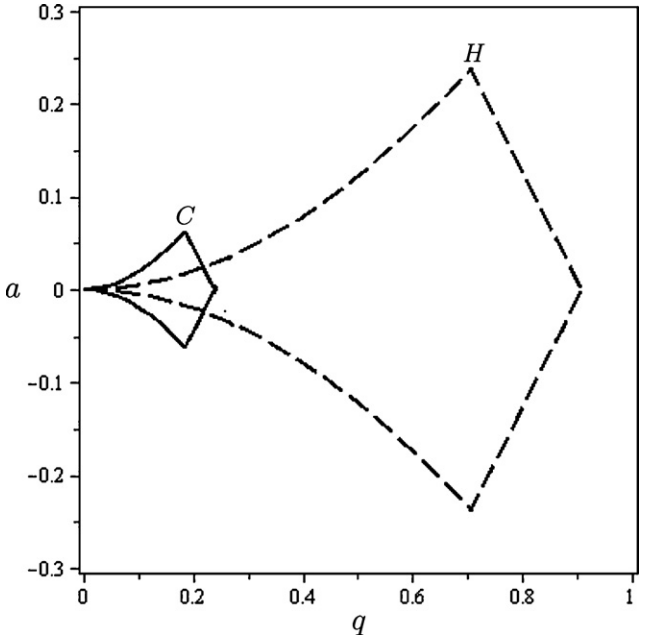

Fig. 3. The first stability regions with $r_{0,1} = r_{0,2} = 10$ (mm), $c_1 = 1$, $c_2 = 3.809$ H: the first stability region for the quadrupole mass filter with hyperbolic rods and C: the first stability region for the quadrupole mass filter with circular rods.

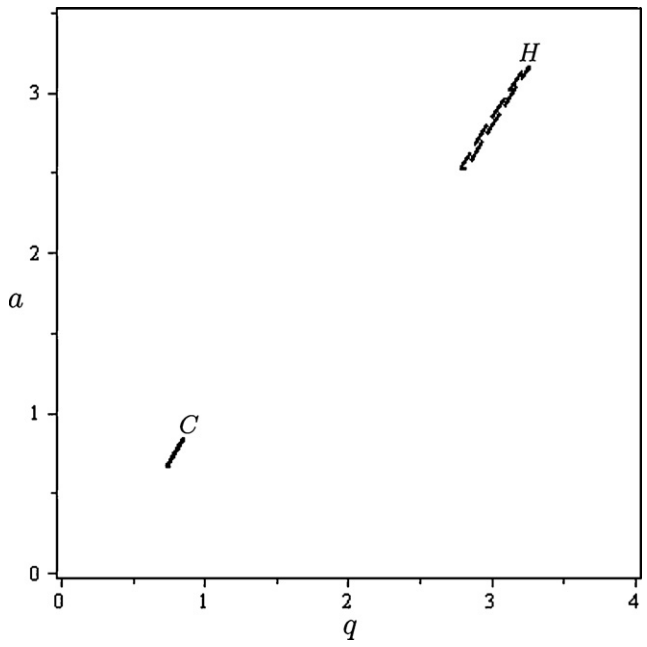

Fig. 4. The second stability regions with $r_{0,1} = r_{0,2} = 10$ (mm), $c_1 = 1$, $c_2 = 3.8099$ *H*: the second stability region for the quadrupole mass filter with hyperbolic rods and *C*: the second stability region for the quadrupole mass filter with circular rods.

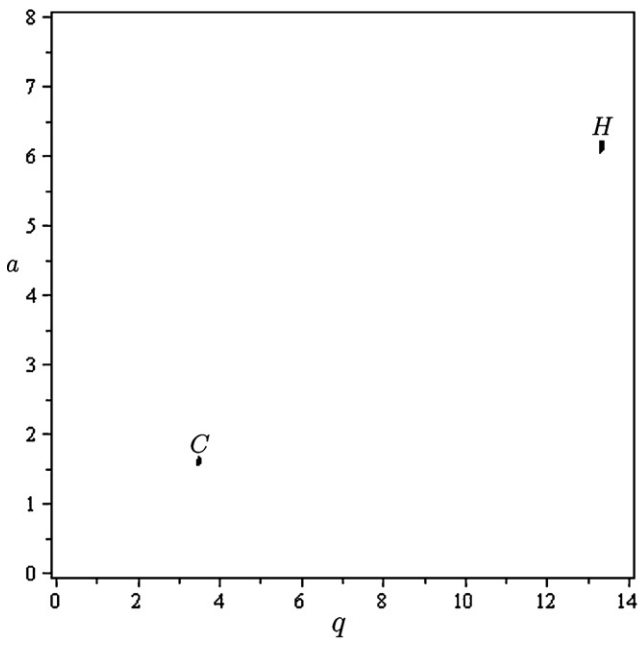

Fig. 6. The fourth stability regions with $r_{0,1} = r_{0,2} = 10$ (mm), $c_1 = 1$, $c_2 = 3.8099$ *H*: the fourth stability region for the quadrupole mass filter with hyperbolic rods and *C*: the fourth stability region for the quadrupole mass filter with circular rods.

To derive Eq. (16) has been used $L = 10$ (cm), $a = 1$ (cm) and $r = 1$ (cm). We waive from some terms in Eq. (16), because they have very small coefficient in compared with another terms. Therefore, considering the terms Eq. (16) only to fourth order approximation, will have as,

$$\Phi(x, y) = c_2\Phi_0(x^2 - y^2); c_2 = 3.8099, \tag{17}$$

which is similar to Eq. (1) with large slope. This equation states that we can apply quadrupole mass filter with round rod electrodes with a good approximation in comparison to ideal case.

In each of the perpendicular directions *x* and *y*, the basic equation of the ion motions of mass *m* and electric charge *e* may be treated independently:

$$\frac{dx^2}{d\zeta^2} + (\alpha_x - 2\chi_x \cos(2\zeta))x = 0, \tag{18}$$

$$\frac{dy^2}{d\zeta^2} - (\alpha_y - 2\chi_y \cos(2\zeta))y = 0 \tag{19}$$

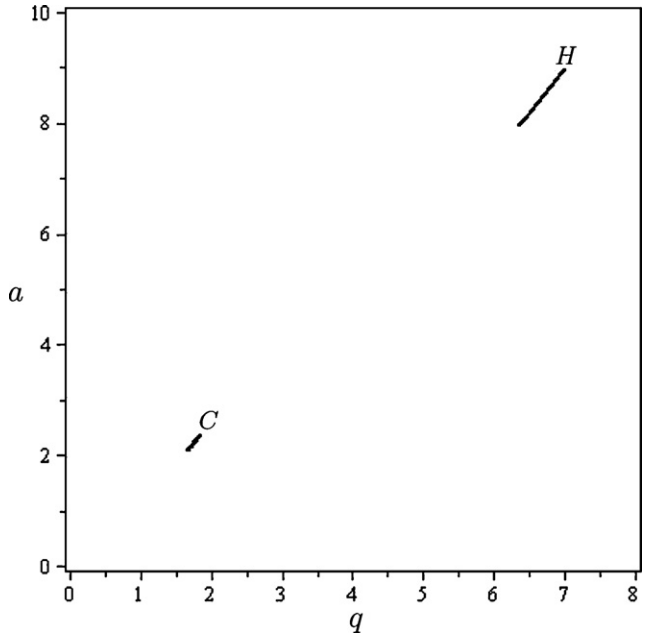

Fig. 5. The third stability regions with $r_{0,1} = r_{0,2} = 10$ (mm), $c_1 = 1$, $c_2 = 3.8099$ *H*: the third stability region for the quadrupole mass filter with hyperbolic rods and *C*: the third stability region for the quadrupole mass filter with circular rods.

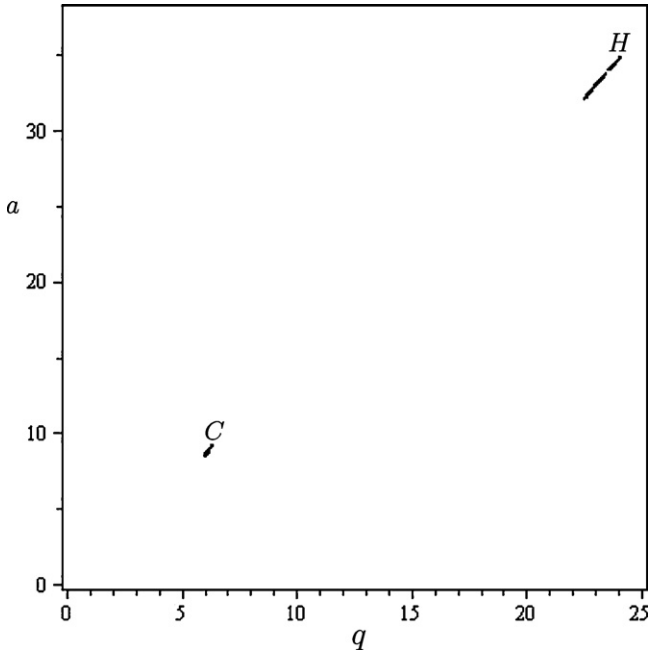

Fig. 7. The fifth stability regions with $r_{0,1} = r_{0,2} = 10$ (mm), $c_1 = 1$, $c_2 = 3.8099$ *H*: the fifth stability region for the quadrupole mass filter with hyperbolic rods and *C*: the fifth stability region for the quadrupole mass filter with circular rods.

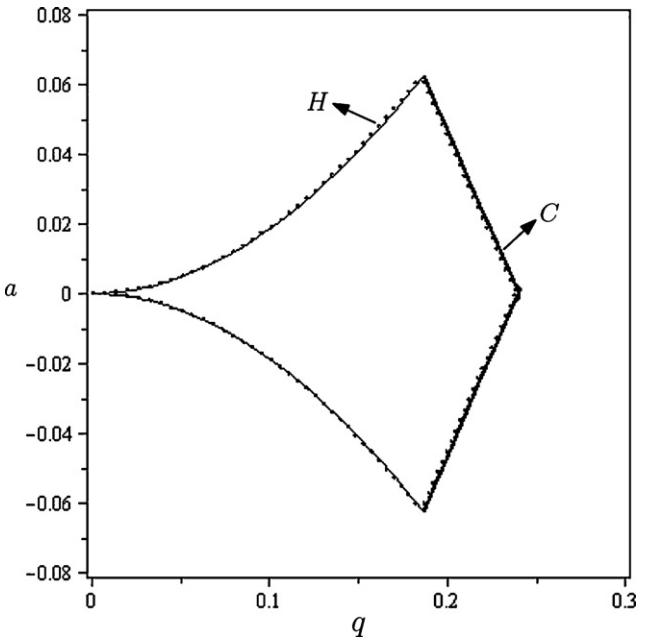

Fig. 8. The first stability regions with $r_{0,1} = 5.14$ (mm), $r_{0,2} = 10$ (mm), $c_1 = 1$, $c_2 = 3.8099$ *H*: the first stability region for the quadrupole mass filter with hyperbolic rods and *C*: the first stability region for the quadrupole mass filter with circular rods.

with the following substitutions:

$$\zeta = \frac{\Omega t}{2}, \alpha_x = -\alpha_y = 8c_2 \frac{e}{m} \times \frac{U_{dc}}{r_{0,2}^2 \Omega^2}, \chi_x = -\chi_y = 4c_2 \frac{e}{m} \times \frac{V_{ac}}{r_{0,2}^2 \Omega^2}, \tag{20}$$

where α_x and χ_x are the trapping parameters.

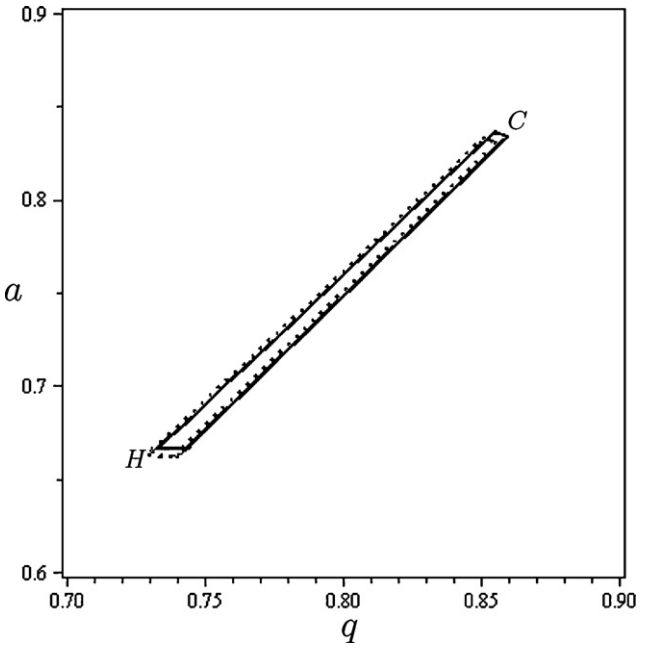

Fig. 9. The second stability regions with $r_{0,1} = 5.14$ (mm), $r_{0,2} = 10$ (mm), $c_1 = 1$, $c_2 = 3.8099$ *H*: the second stability region for the quadrupole mass filter with hyperbolic rods and *C*: the second stability region for the quadrupole mass filter with circular rods.

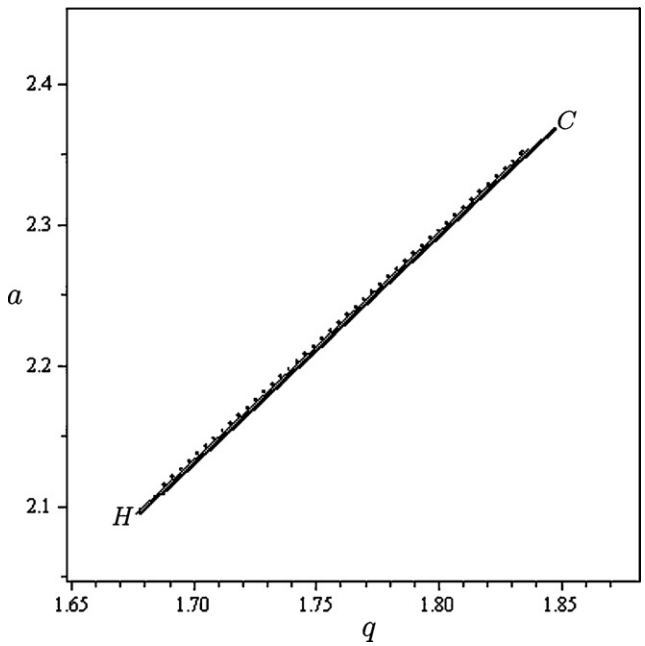

Fig. 10. The third stability regions with $r_{0,1} = 5.14$ (mm), $r_{0,2} = 10$ (mm), $c_1 = 1$, $c_2 = 3.8099$ *H*: the third stability region for the quadrupole mass filter with hyperbolic rods and *C*: the third stability region for the quadrupole mass filter with circular rods.

3.1. Expression of trapping parameters

If we consider ions of the same species and if it applies to both type of cages potential difference of same amplitude and same frequency, then we have the following relationship between the parameters α_x and χ_x on one side and a_x and q_x other hand:

$$\frac{\alpha_x}{a_x} = \frac{r_{0,1}^2}{r_{0,2}^2} \times \frac{c_2}{c_1} \text{ and } \frac{\chi_x}{q_x} = \frac{r_{0,1}^2}{r_{0,2}^2} \times \frac{c_2}{c_1}. \tag{21}$$

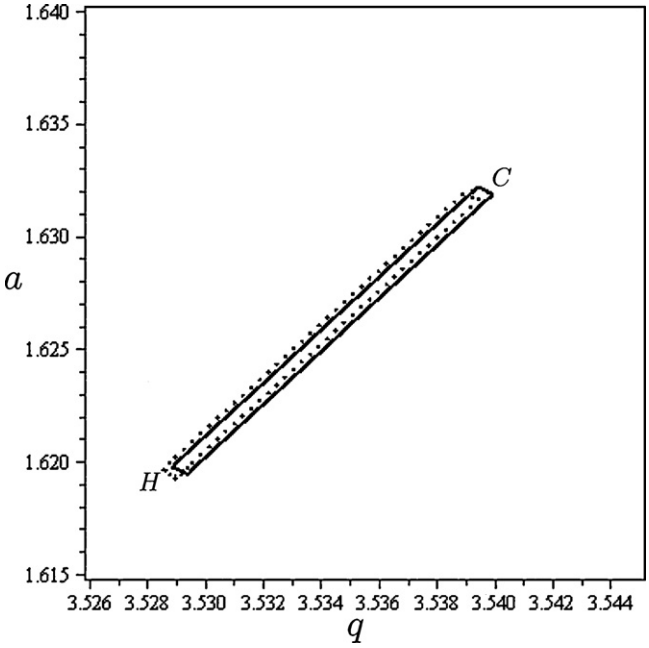

Fig. 11. The fourth stability regions with $r_{0,1} = 5.14$ (mm), $r_{0,2} = 10$ (mm), $c_1 = 1$, $c_2 = 3.8099$ *H*: the fourth stability region for the quadrupole mass filter with hyperbolic rods and *C*: the fourth stability region for the quadrupole mass filter with circular rods.

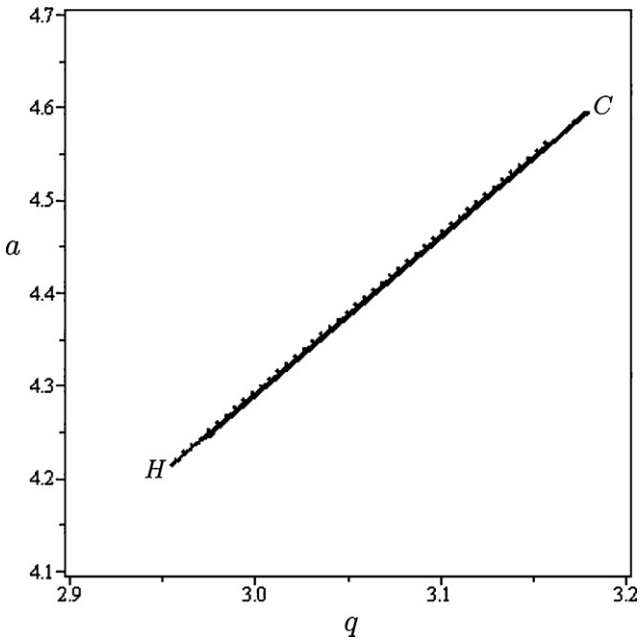

Fig. 12. The fifth stability regions with $r_{0,1} = 5.14$ (mm), $r_{0,2} = 10$ (mm), $c_1 = 1$, $c_2 = 3.8099$ *H*: the fifth stability region for the quadrupole mass filter with hyperbolic rods and *C*: the fifth stability region for the quadrupole mass filter with circular rods.

From Eq. (21) we have

$$\alpha_x = \left(\frac{r_{0,1}}{r_{0,2}}\right)^2 \left(\frac{c_2}{c_1}\right) a_x \text{ and } \chi_x = \left(\frac{r_{0,1}}{r_{0,2}}\right)^2 \left(\frac{c_2}{c_1}\right) q_x. \quad (22)$$

4. Results

4.1. Stability regions

To compute the accurate elements of the motion equations for the stability diagrams, a fifth order Runge–Kutta method is employed. Figs. 3–12 present the calculated stability regions I until V for the quadrupole mass filter with hyperbolic rods and quadrupole mass filter with circular rods for $r_{0,1} = r_{0,2} = 10$ (mm), $c_1 = 1$, $c_2 = 3.8099$ and $r_{0,1} = 5.14$ (mm), $r_{0,2} = 10$ (mm), $c_1 = 1$, $c_2 = 3.8099$, respectively using 0.001 steps increment in fifth order Runge–Kutta method.

Figs. 3–7 show that the stability regions I until V for quadrupole mass filter with circular rods are miniaturized and shifted. Figs. 8–12 show that the stability regions I until V for quadrupole mass filter with circular rods are shifted. Table 1 shows the values of (a_x, q_x) at the lower and upper tips of the five stability regions of a quadrupole mass filter with hyperbolic rods for $c_1 = 1$, $r_{0,1} = 10$ (mm). Tables 2 and 3 show the values of (α_x, χ_x) at the lower and upper tips of the five stability regions of a quadrupole mass filter with circular rods for $c_2 = 3.8099$, $r_{0,2} = 10$ (mm) and $c_2 = 3.8099$, $r_{0,2} = 5.14$ (mm), respectively.

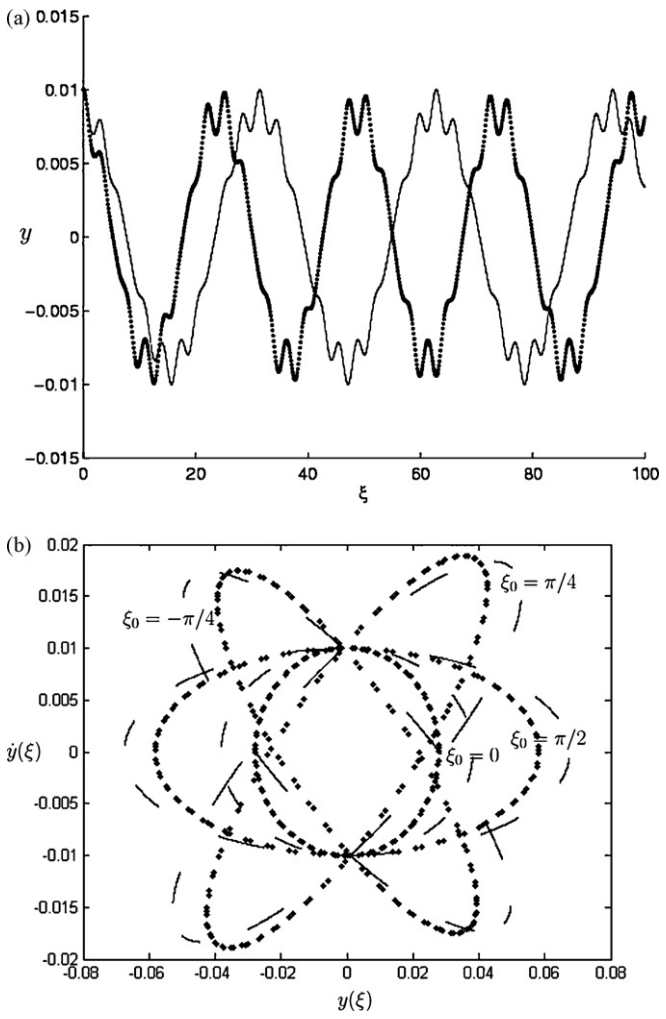

Fig. 13. (a): Ion trajectories in real time for $\beta_y = 0.2$ and (b): evolution of the phase space ion trajectory for different values of the phase ξ_0 for $\beta_y = 0.2$, dash line: for quadrupole mass filter with hyperbolic rods for $c_1 = 1$, $r_{0,1} = 10$ (mm), dot line: for quadrupole mass filter with circular rods for $c_2 = 3.8099$, $r_{0,2} = 10$ (mm).

Table 1
The values of a_x and q_x at the lower and upper tips of the five stability regions of a quadrupole mass filter with hyperbolic rods for $c_1 = 1$, $r_{0,1} = 10$ (mm).

	a_x		q_x	
Region no.	Lower tip	Upper tip	Lower tip	Upper tip
I	−0.243	0.243	0.000	0.910
II	2.521	3.162	2.771	3.253
III	7.983	8.961	6.381	6.990
IV	6.134	6.181	13.360	13.402
V	16.072	17.393	11.261	12.031

Table 2
The values of α_x and χ_x at the lower and upper tips of the five stability regions of a quadrupole mass filter with circular rods for $c_2 = 3.8099$, $r_{0,2} = 10$ (mm).

	α_x		χ_x	
Region no.	Lower tip	Upper tip	Lower tip	Upper tip
I	−0.061	0.061	0.000	0.242
II	0.673	0.841	0.732	0.861
III	2.113	2.371	1.694	1.852
IV	1.623	1.632	3.529	3.541
V	4.248	4.595	2.982	3.181

Table 3
The values of α_x and χ_x at the lower and upper tips of the five stability regions of a quadrupole mass filter with circular rods for $c_2 = 3.8099$, $r_{0,2} = 5.14$ (mm).

	α_x		χ_x	
Region no.	Lower tip	Upper tip	Lower tip	Upper tip
I	−0.063	0.063	0.000	0.241
II	0.661	0.834	0.728	0.862
III	2.093	2.364	1.681	1.847
IV	1.613	1.628	3.515	3.527
V	4.233	4.582	2.967	3.175

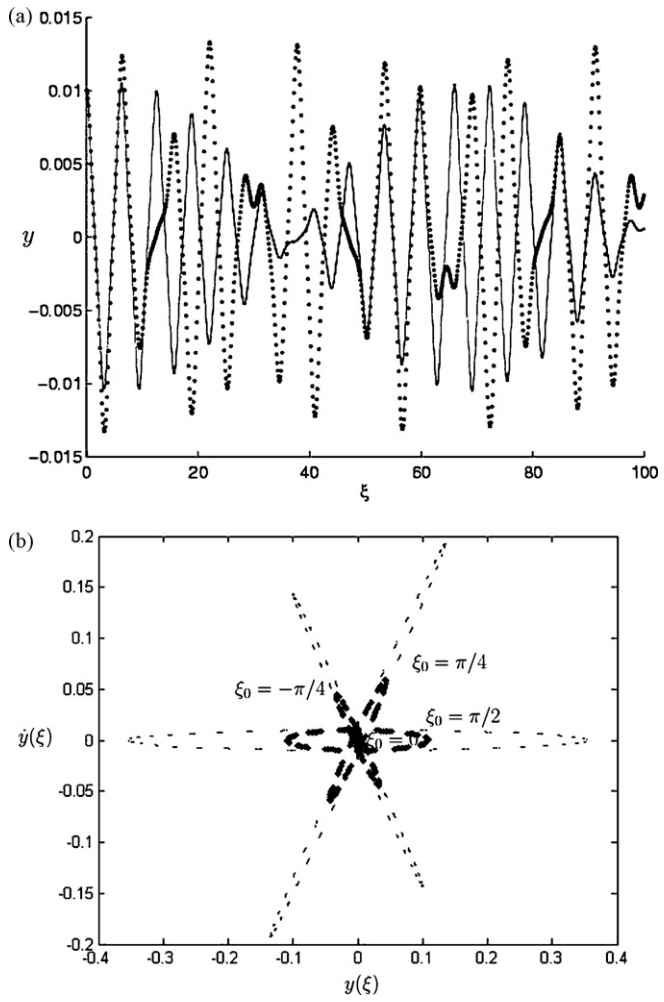

Fig. 14. (a): Ion trajectories in real time for $\beta_y = 0.95$ and (b): evolution of the phase space ion trajectory for different values of the phase ξ_0 for $\beta_y = 0.95$, dash line: for quadrupole mass filter with hyperbolic rods for $c_1 = 1$, $r_{0,1} = 10$ (mm), dot line: for quadrupole mass filter with circular rods for $c_2 = 3.8099$, $r_{0,2} = 10$ (mm).

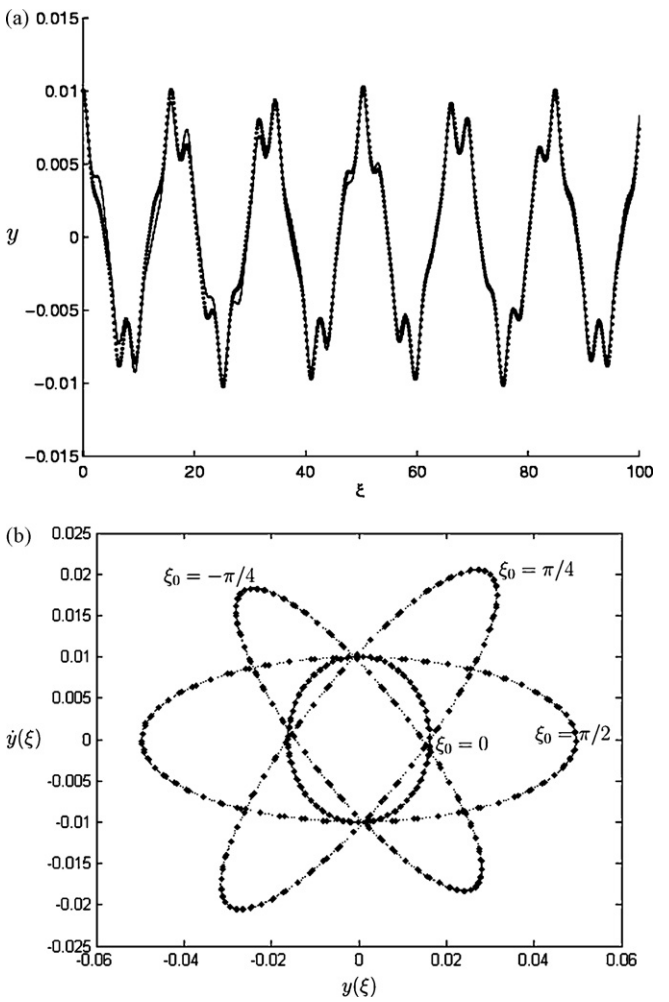

Fig. 15. (a): Ion trajectories in real time for $\beta_y = 0.3$ and (b): evolution of the phase space ion trajectory for different values of the phase ξ_0 for $\beta_y = 0.3$, dash line: for quadrupole mass filter with hyperbolic rods for $c_1 = 1$, $r_{0,1} = 5.14$ (mm), dot line: for quadrupole mass filter with circular rods for $c_2 = 3.8099$, $r_{0,2} = 10$ (mm).

4.2. Ion trajectories

The properties of the confined ions in the quadrupole mass filter with hyperbolic rods and quadrupole mass filter with circular rods were examined through ion displacement and presented both in real time and in x, y space. For this aim, the operating points, four operating points located in their corresponding stability diagram having the same β_y, in the first stability diagrams of the quadrupole mass filter with hyperbolic rods and quadrupole mass filter with circular rods for different values, $c_1 = 1$, $r_{0,1} = 10$ (mm), $c_1 = 1$, $r_{0,1} = 5.14$ (mm) and $c_2 = 3.8099$, $r_{0,2} = 10$ (mm), $c_2 = 3.8099$, $r_{0,2} = 10$ (mm), respectively.

The operating points used as follows: $\beta_y = 0.2$, $a_x = 0$, $q_x = 0.2784$ for quadrupole mass filter with hyperbolic rods with $c_1 = 1$, $r_{0,1} = 10$ (mm) and $\alpha_x = 0$, $\chi_x = 0.0923$ for quadrupole mass filter with circular rods with $c_2 = 3.8099$, $r_{0,2} = 10$ (mm), $\beta_y = 0.95$, $a_x = 0$, $q_x = 0.9052$ for quadrupole mass filter with hyperbolic rods with $c_1 = 1$, $r_{0,1} = 10$ (mm) and $\alpha_x = 0$, $\chi_x = 0.2490$ for quadrupole mass filter with circular rods with $c_2 = 3.8099$, $r_{0,2} = 10$ (mm), $\beta_y = 0.3$, $a_x = 0$, $q_x = 0.1318$ for quadrupole mass filter with hyperbolic rods with $c_1 = 1$, $r_{0,1} = 5.14$ (mm) and $\alpha_x = 0$, $\chi_x = 0.1310$ for quadrupole mass filter with circular rods with $c_2 = 3.8099$, $r_{0,2} = 10$ (mm) and $\beta_y = 0.97$, $a_x = 0$, $q_x = 0.2505$ for quadrupole mass filter with hyperbolic rods with $c_1 = 1$, $r_{0,1} = 5.14$ (mm) and $\alpha_x = 0$, $\chi_x = 0.2489$ for quadrupole mass filter with circular rods with $c_2 = 3.8099$, $r_{0,2} = 10$ (mm). Table 4 shows the values of q_x and χ_x for the quadrupole mass filter with hyperbolic rods for $c_1 = 1$, $r_{0,1} = 10$ (mm) and quadrupole mass filter with circular rods for $c_2 = 3.8099$, $r_{0,2} = 10$ (mm), respectively, for $\beta_y = 0.2;0.5;0.95$ and Table 5 shows the values of q_x

Table 4
The values of q_x and χ_x for the quadrupole mass filter with hyperbolic rods for $c_1 = 1$, $r_{0,1} = 10$ (mm) and quadrupole mass filter with circular rods for $c_2 = 3.8099$, $r_{0,2} = 10$ (mm), respectively, for $\beta_y = 0.2;0.5;0.95$.

β_y	q_x	χ_x
	Quadrupole mass filter with hyperbolic rods	Quadrupole mass filter with circular rods
0.2	0.2784	0.0923
0.5	0.6393	0.1926
0.95	0.9052	0.2490

Table 5
The values of q_x and χ_x for the quadrupole mass filter with hyperbolic rods for $c_1 = 1$, $r_{0,1} = 5.14$ (mm) and quadrupole mass filter with circular rods for $c_2 = 3.8099$, $r_{0,2} = 10$ (mm), respectively, for $\beta_y = 0.3;0.6;0.97$.

β_y	q_x	χ_x
	Quadrupole mass filter with hyperbolic rods	Quadrupole mass filter with circular rods
0.3	0.1318	0.1310
0.6	0.2165	0.2151
0.97	0.2505	0.2489

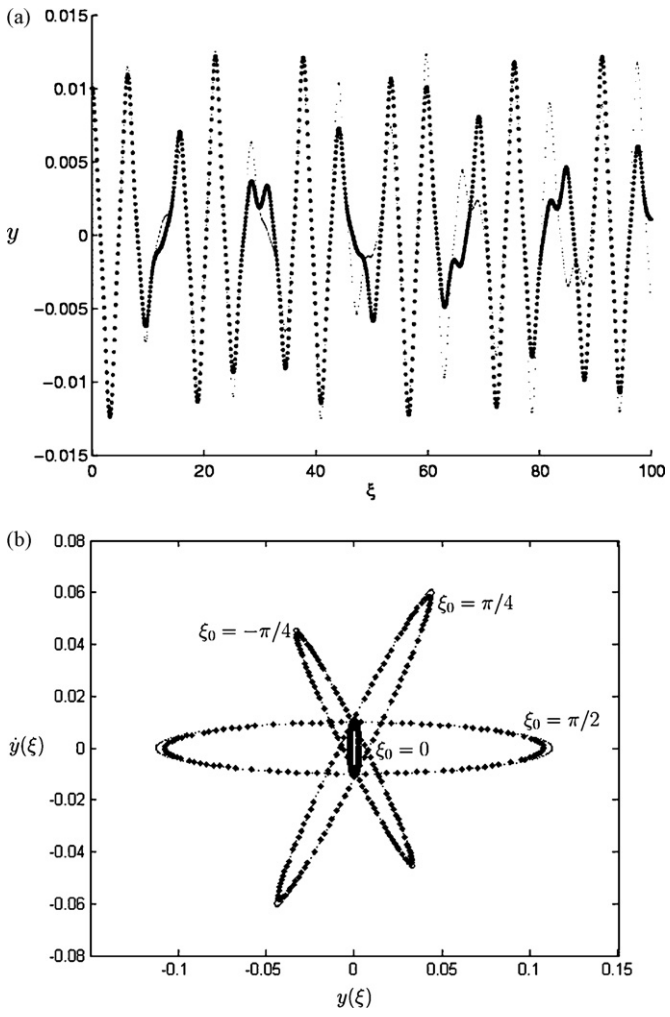

Fig. 16. (a): Ion trajectories in real time for $\beta_y = 0.97$ and (b): evolution of the phase space ion trajectory for different values of the phase ξ_0 for $\beta_y = 0.97$, dash line: for quadrupole mass filter with hyperbolic rods for $c_1 = 1$, $r_{0,1} = 5.14$ (mm), dot line: for quadrupole mass filter with circular rods for $c_2 = 3.8099$, $r_{0,2} = 10$ (mm).

and χ_x for the quadrupole mass filter with hyperbolic rods for $c_1 = 1$, $r_{0,1} = 5.14$ (mm) and quadrupole mass filter with circular rods for $c_2 = 3.8099$, $r_{0,2} = 10$ (mm), respectively, for $\beta_y = 0.3;0.6;0.97$.

Fig. 13.(a), Fig. 14.(a), Fig. 15.(a) and Fig. 16.(a) shows the ion trajectories in real time with $\beta_y = 0.2, 0.95$ when $c_1 = 1$, $r_{0,1} = 10$ (mm), $c_2 = 3.8099$, $r_{0,2} = 10$ (mm) and $\beta_y = 0.3, 0.97$ when $c_1 = 1$, $r_{0,1} = 5.14$ (mm), $c_2 = 3.8099$, $r_{0,2} = 10$ (mm). Fig. 13.(b), Fig. 14.(b), Fig. 15.(b) and Fig. 16.(b) shows the evolution of the phase space ion trajectory for different values of the phase ξ_0 for $\beta_y = 0.2, 0.95$ when $c_1 = 1$, $r_{0,1} = 10$ (mm), $c_2 = 3.8099$, $r_{0,2} = 10$ (mm) and $\beta_y = 0.3, 0.97$ when $c_1 = 1$, $r_{0,1} = 5.14$ (mm), $c_2 = 3.8099$, $r_{0,2} = 10$ (mm).

Fig. 15(a) and Fig. 16 shows that, for the same equivalent operating point in two stability diagrams (having the same $\beta_y = 0.3, 0.97$) the associated modulated secular ion frequencies behavior are the same for the suitable parameters $c_1 = 1$, $r_{0,1} = 5.14$ (mm), $c_2 = 3.8099$ and $r_{0,2} = 10$ (mm).

5. Discussion and conclusion

The behavior of a quadrupole mass filter with hyperbolic rods and quadrupole mass filter with circular rods has been demonstrated. The more important result of this paper show that, for the same equivalent operating point in two stability diagrams (having the same $\beta_y = 0.3, 0.97$) the associated modulated secular ion frequencies behavior are the same for the suitable parameters $c_1 = 1$, $r_{0,1} = 5.14$ (mm), $c_2 = 3.8099$ and $r_{0,2} = 10$ (mm). Therefore, optimum rod size for quadrupole mass filter with circular rods to take same results compared with quadrupole mass filter with hyperbolic rods is $r_{0,2} = 1.9455 r_{0,1}$. Here, $r_{0,2}$ is hyperbolic rods radius and $r_{0,1}$ is circular rods radius.

References

[1] P.H. Dawson, Quadrupole Mass Spectrometry and its Applications, AIP Press, N.Y., 1995.
[2] P.H. Dawson, N.R. Whetten, J. Vac. Sci. Technol. 7 (1970) 440.
[3] D.R. Denison, J. Vac. Sci. Technol. 8 (1971) 266.
[4] H. Matsuda, T. Matsuo, Int. J. Mass Spectrom. Ion Phys. 24 (1977) 107.
[5] G.R. Janik, J.D. Prestage, L. Maleki, J. App. Phys. 67 (1990) 6050.
[6] J. Schulte, P.V. Shevchenko, A.V. Radchik, Rev. Sci. Instrum. 70 (1999) 3566.
[7] S. Seddighi Chaharborj, S.M. Sadat Kiai, J. Mass Stectrom. 45 (2010) 1111.
[8] A.L. Michaud, A.J. Frank, C. Ding, X. Zhao, D.J. Douglas, J. Am. Soc. Mass Spectrom. 16 (2005) 835.
[9] N. Konenkov, F. Londry, C. Ding, D.J. Douglas, J. Am. Soc. Mass Spectrom. 17 (2006) 1063.
[10] W. Paul, H. Steinwedel, Z. Naturforch. 8a (1953) 448.
[11] N.W. McLachlan, Theory and Application of Mathieu Functions, Dover Publications, 1964.